

Poor scaling between elastic energy release and eruption intensity at Tungurahua Volcano, Ecuador

Jeffrey B. Johnson,¹ Mario C. Ruiz,^{2,3} Jonathan M. Lees,² and Patricio Ramon³

Received 27 February 2005; revised 6 June 2005; accepted 28 June 2005; published 4 August 2005.

[1] An important objective in volcanology is the quantification of eruption intensity through the study of elastic energy propagated into the atmosphere and ground. To better understand the relation between elastic wave radiation and eruptive activity we deployed seismic, acoustic, and video instrumentation at the active Tungurahua Volcano (Ecuador) in Nov.–Dec. of 2004. Our data show that plume expansion scales very poorly with both seismic and acoustic trace energy and only the initial amplitude of the acoustic signal is perhaps correlated with initial plume rise speeds. In general, the eventual size of Tungurahua eruption plumes does not appear to be controlled by elevated material accelerations within the conduit, which are primary influences on elastic energy radiation. This result has vital implications for volcano observatories, which are interested in using seismic and acoustic trace amplitudes as proxies for eruption magnitudes.

Citation: Johnson, J. B., M. C. Ruiz, J. M. Lees, and P. Ramon (2005), Poor scaling between elastic energy release and eruption intensity at Tungurahua Volcano, Ecuador, *Geophys. Res. Lett.*, *32*, L15304, doi:10.1029/2005GL022847.

1. Introduction

[2] Many volcanoes worldwide radiate substantial seismic and infrasonic energy coincident with explosive degassing. In simple cases, such as at Mount Erebus, discrete Strombolian-type explosions are associated with the bursting of large overpressurized gas slugs at the lava lake free surface [Dibble *et al.*, 1984]. Here the bubble rupture coincides with the initiation of both short period seismicity and infrasound (i.e., sound <20 Hz). Because seismic and acoustic energy scales well with each other for relatively large Erebus explosions [Rowe *et al.*, 2000], it is probable that larger bubble bursts or higher initial gas pressures simultaneously radiate more seismo-acoustic energy into the respective media.

[3] However, a clear correlation between seismic and acoustic intensity is not apparent at many other episodically-erupting volcanoes (e.g., Arenal [Garces *et al.*, 1998; Hagerty *et al.*, 2000], Karymsky [Johnson and Aster, 2005], and Santiaguito [Johnson *et al.*, 2004]). Moreover, for small-scale explosions common at Karymsky [Johnson, 2000] and Santiaguito [Johnson *et al.*, 2004], where additional

video and thermal observations have been made, it appears as though only acoustic intensity, not seismic intensity is related to initial muzzle velocity and/or initial plume rise speeds. The observed relation is attributed to explosive material emissions from a fragmentation source with an open-vent configuration. Unimpeded shallow-conduit sources perturb the atmosphere through explosive gas expansion, which efficiently generates high-amplitude, long-period acoustic waves [Lighthill, 1978].

[4] Seismic amplitudes, on the other hand, seem to exhibit poor scaling with muzzle velocity, plume expansion rate, or eventual plume size. Comparative studies between seismic radiation and eruption intensity for suites of discrete explosions at both Karymsky [Johnson, 2000] and Santiaguito [Johnson *et al.*, 2004] failed to reveal a robust relation. In another study comparing seismic tremor amplitudes with ash column heights at 14 different volcanoes [McNutt, 1994], a clear relation was also not evident for smaller eruptions (i.e., plume heights < ~2 km). Discrete explosion seismicity and tremor may reflect somewhat differing source mechanisms, but small-scale eruptions, which manifest both transient seismicity and short-duration tremor, are common worldwide and are endemic at many volcanoes (e.g., Karymsky, Santiaguito, and Tungurahua). Our inability to assess the magnitude of small eruptions using seismic trace data leads to a general difficulty in remote assessment of small-magnitude eruptive activity presenting problems for those engaged in volcano monitoring (e.g., at Tungurahua, IG-EPN, personal communication, 2004; at Volcán de Colima, N. Varley, personal communication, 2004).

2. Background and Experiment

[5] Tungurahua was selected for an integrated seismo-acoustic-video study because of the reliability and diversity of its eruptive activity. Located in the southern portion of the Ecuadorian Cordillera Real, this andesitic stratovolcano is historically extremely active [Hall *et al.*, 1999]. Since Oct. 1999 and prior to Mar. 2005 the volcano has been in a nearly continuous state of explosive degassing with only a few month-long periods of relative repose (a chronology of activity is published in IG-EPN reports available online in Spanish at: <http://www.igepn.edu.ec/vulcanologia/tungurahua/actividad/informet.htm>). Since early 2000, eruption intensity has been generally diminished from the vigorous Vulcanian-type activity characteristic of the 1999 eruption onset. Recent activity (e.g., winter 2004–2005) comprises discrete explosive events generating columns up to 3 km, smaller-scale Strombolian-type emissions, and passive, a-seismic degassing, which feeds an intermittent SO₂-rich plume.

¹Department of Earth Sciences, University of New Hampshire, Durham, New Hampshire, USA.

²Department of Geological Sciences, University of North Carolina, Chapel Hill, North Carolina, USA.

³Instituto Geofísico, Escuela Politécnica Nacional (IG-EPN), Quito, Ecuador.

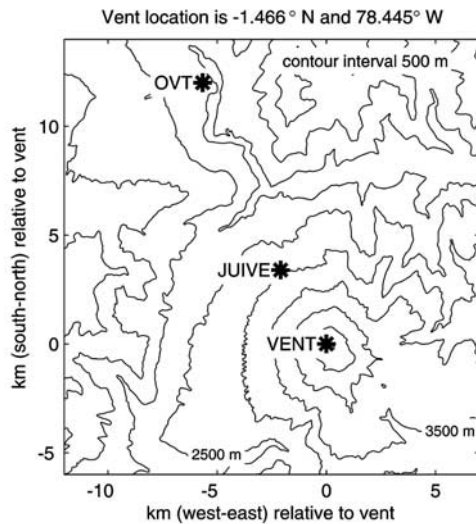


Figure 1. Relative locations of vent, JUIVE seismo-acoustic station, and OVT video camera.

[6] Our experiment in Nov.–Dec. of 2004 captured activity during the waning portion of one of Tungurahua’s characteristic eruptive cycles. Our seismo-acoustic installation was similar to one deployed in Jun.–Aug. of 2004 [Ruiz *et al.*, 2005], which recorded activity during the apex of the same eruptive cycle. In the Nov.–Dec. experiment, deployed sensors included two co-located Larson-Davis electret condenser microphones (corner at 0.27 Hz) and a 3-component CMG-40T (30 s) broadband seismometer. These sensors re-occupied station JUIVE, located ~ 4200 m from the inferred vent (Figure 1). Data acquisition to a 6-channel Reftek 130 was continuous at 125 Hz between Nov. 20 and Dec. 15.

[7] A SONY DCR-VX2000 video camera was operated at the Observatorio Volcanológico Tungurahua (OVT), 13.5 km from the vent. During the project, weather conditions were decent, allowing for successful video acquisition of many explosive events during periods of zero cloud cover. From OVT, the camera was inclined at 12° , providing low angular distortion for vertically-rising plumes. Using the optical zoom, the camera focused on a ~ 1000 m \times ~ 800 m field-of-view centered on a ~ 500 m horizontal portion of the crater rim. We operated the camera continuously during good weather and synchronized the internal clock with GPS daily such that timing is accurate to within ± 0.5 s.

3. Analysis

[8] During periods of decent weather, all video footage was thoroughly reviewed. Events for which the onsets of explosive emissions were clearly visible were selected and windowed. In total, ~ 20 such events were identified during ~ 10 hours of good weather. However, only 6 of these events were associated with clear acoustic or seismic transients and occurred during periods of low wind (i.e., plume rising vertically). In this study we compare acoustic and seismic radiation associated with 4 events that produced plumes of relatively similar size.

[9] In Figure 2 still images are depicted at 10 s intervals to quantify the evolution of plume expansion over time.

Seismic and acoustic trace data were windowed to match the video events and then time-shifted to represent approximate origin times at the vent (Figure 2). Assuming reasonable atmospheric sound speeds of 320 m/s $\pm 2.5\%$, P-wave seismic velocities of 2500 m/s $\pm 25\%$ (I. Molina, personal communication, 2004), and a source-receiver slant distance of 4200 m $\pm 2.5\%$ for a shallow (< 500 m deep) conduit source, seismic and acoustic origin times may be estimated. Acoustic transients are thus assumed to be generated $\sim 13 \pm 0.7$ s prior to their arrival at JUIVE and seismic generation is $\sim 1.8 \pm 0.2$ s prior to first arrival picks. Thus in Figure 2, acoustic and seismic traces have been time-shifted 13 s and 2 s respectively, resulting in approximate time origins for both the emergent seismic and impulsive acoustic onsets. These onsets are coincident to within the margin of seismic picking error ($< \pm 1$ s) indicating a nearly-synchronous seismo-acoustic source perturbation. Acoustic origin times may be separately confirmed from select video records (e.g., event #1; example in the auxiliary material), in which initial shocks induce temporary condensation of clouds near the vent. These visible shocks occur within $+1$ s of the inferred seismo-acoustic origin time within the conduit.

[10] We estimate origin time uncertainties of about ± 1 s for the seismo-acoustic source and ± 0.5 s for the video records, which allow us to constrain timing relations for the different events. The first image in each sequence of Figure 2 corresponds to the initial appearances of a dark (ash-rich) plume rising above the lip of the crater rim. In these frames, the plume has already risen a finite distance before it is visible to the camera. For events #1–4, inferred seismo-acoustic origin times precedes plume appearance on the video by 2, 6, 5, and 9 s respectively. These delays can be attributed either to variable source depth, indicating fluctuating acoustic source locations within a conduit, and/or to variable initial plume rise velocity [e.g., Hagerty *et al.*, 2000; Ripepe *et al.*, 2001]. Based upon systematic variations in delay times between seismic and acoustic phases Ruiz *et al.* [2005] speculate that Tungurahua events may emanate from variable source depths.

[11] For the 4 explosions presented here seismo-acoustic origin times appear nearly synchronous. Thus a fixed fragmentation depth and variable plume rise velocity could adequately explain the data. For instance, the explosion with largest acoustic amplitude (event #1) exhibits the shortest delay time (~ 2 s) between the inferred seismo-acoustic source origin time and plume appearance. This short delay time would be expected if the initial material ejection occurs with great acceleration (i.e., high initial muzzle velocity).

[12] The areal extent of the growing plume in the video is used to estimate evolving plume volume. At volcano observatories it is often plume size that serves as a qualitative proxy of eruption magnitude. Following simplifications to Chouet *et al.* [1974], we estimate plume volume from the video stills assuming cylindrical symmetry about the z -axis and a vertically rising plume. Plume volume V is thus estimated as: $V = \pi/4 \int_{z=\text{vent}}^{z=\text{top}} D(z)^2 dz$, where D is the plume horizontal dimension, which varies as a function of height. Assuming low winds, which appears to be the case for the Figure 2 events, volumetric plume growth can be roughly assessed as a function of time. The plume evolution may then be compared to the radiated seismic and acoustic signals.

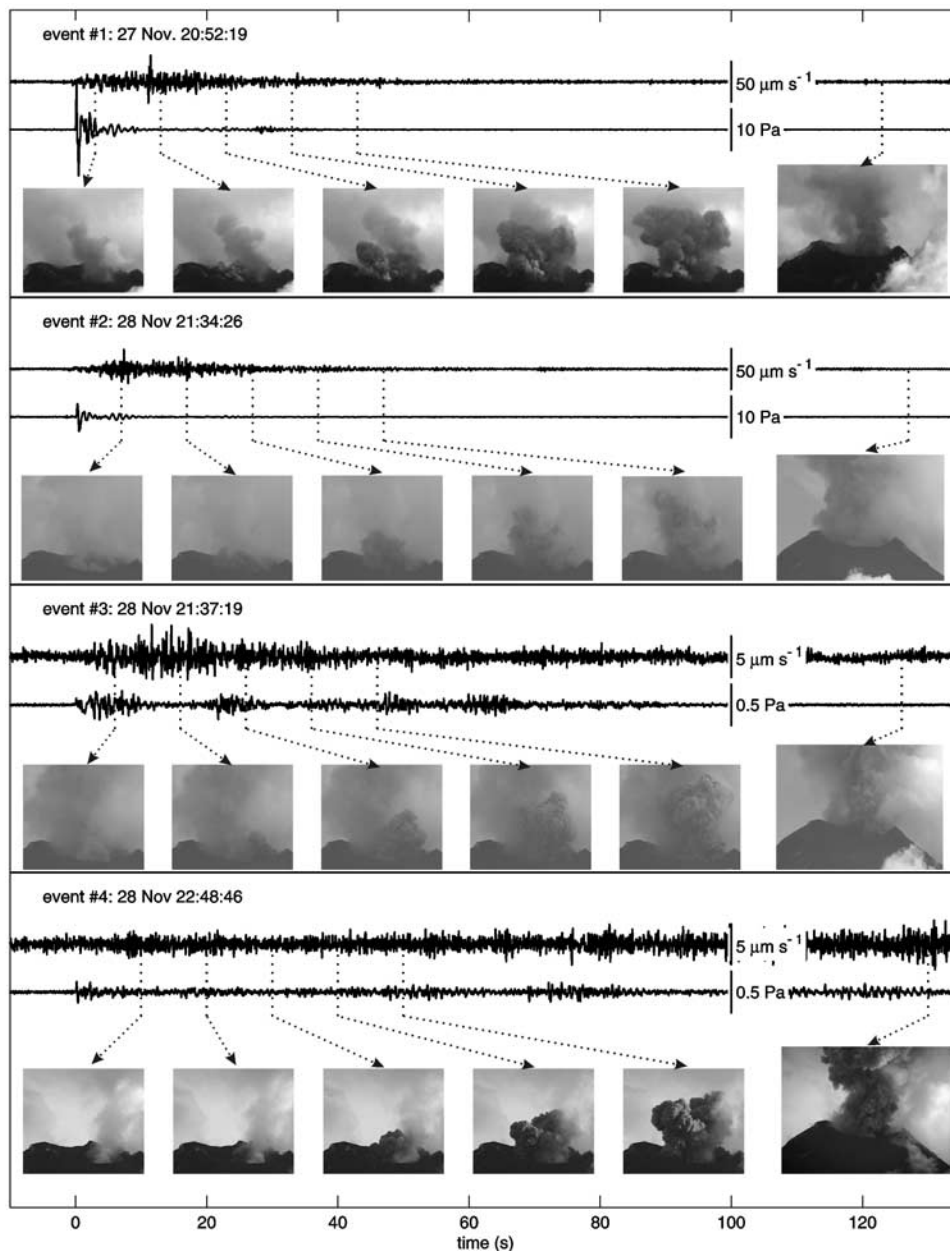


Figure 2. Time-shifted seismic velocity traces, acoustic pressure traces, and video still images for 4 select eruptive events at Tungurahua. Timing of image frames is indicated by the vertical lines. Note that amplitude scales are decreased for events #3 and 4 relative to events #1 and 2. Original mpeg video clips from these events are available in the auxiliary material¹.

[13] To discover a relation between elastic energy and plume growth, we attempt to quantify seismic and acoustic strength by assessing both amplitude and energy for the 4 events (Table 1). We measure both the maximum peak-to-peak seismic displacement (A_S) and peak-to-peak acoustic pressure traces (A_A) occurring within specified time intervals (i.e., during the first 10 s, 60 s, and 120 s). For energy, we calculate the integrated squared velocity trace $U(t)$ and excess pressure trace $\Delta P(t)$ during fixed time intervals (first 10 s, 60 s, and 120 s): $E_S \propto \int U(t)^2 dt$ and $E_A \propto \int \Delta P(t)^2 dt$ [after Johnson and Aster, 2005]. For seismic energy, it is important to note that propagation effects, including scattering and superposition of wave types, will cause signals to be extended in time. For both seismic and acoustic energy,

care is taken to calculate elastic energies for events with low environmental noise. Acoustic data are left unfiltered, but seismic data are high-pass filtered (>0.2 Hz) prior to their conversion to displacement. Tabulated amplitudes and energies are calculated and shown for three different time intervals (first 10 s, 60 s, and 120 s after signal onset). All seismic and acoustic values are time-shifted and normalized for comparison. Average plume growth rate is calculated only at 10 s and 60 s because the plume has extended beyond the field of view at 120 s. It is critical to note that

¹Auxiliary material is available at <ftp://ftp.agu.org/apend/gl/2005GL022847>.

Table 1. Seismo-Acoustic-Video Statistics for the 4 Tungurahua Explosions^a

Event	Seismic		Acoustic		Video, $\times 10^6$ m ³
	A_S	E_S	A_A	E_A	
			<i>At 10 s</i>		
#1	1	1	1	1	2.0
#2	1.7	0.9	0.3	0.1	4.0
#3	0.17	0.02	0.01	0.001	1.5
#4	0.13	0.01	0.01	0.0003	1.5
			<i>At 60 s</i>		
#1	1	1	1	1	70
#2	0.7	0.6	0.3	0.1	30
#3	0.11	0.04	0.02	0.002	50
#4	0.06	0.02	0.01	0.0009	40
			<i>At 120 s</i>		
#1	1	1	1	1	...
#2	0.7	0.6	0.3	0.1	...
#3	0.11	0.05	0.02	0.003	...
#4	0.09	0.05	0.01	0.002	...

^aColumns 2–5: Normalized peak-to-peak seismic displacement amplitudes (A_S), seismic energies (E_S), peak-to-peak acoustic pressure amplitudes (A_A), and acoustic energies (E_A) at 10, 60, and 120 s. Column 6: inferred plume volumes (V) at 10 and 60 s.

despite relatively consistent plume volumes, there exists two orders of magnitude variation in seismic energy and three orders of magnitude variation in acoustic energy for the 4 displayed events.

4. Discussion

[14] This study demonstrates that Tungurahua plume growth, which is often taken as a proxy for eruption intensity, does not scale well with either seismic or acoustic strength. Although plume expansion is dependent upon many factors, including thrust region size, atmospheric conditions, and pyroclast and volatile content [Sparks, 1997], we have highlighted video from 4 similarly-behaved plumes. Despite similar sizes, these events exhibit dramatic differences in their elastic energy radiation (seismic and acoustic intensity for events #3 and 4 is less than 10% of events #1 and 2). It may be noteworthy that the time duration of the seismo-acoustic traces for events #3 and 4 is extended. Despite their consistently lower amplitudes, the extended duration of these signals suggests continuing thrusting in the conduit, which feeds the plume. This is especially evident in event #4, which despite almost no seismic signature, is still emitting 120 s after the eruption onset. This suggests that seismo-acoustic amplitudes are not suitable indicators of size for these types of eruptions.

[15] The important question stands: “What do seismo-acoustic amplitudes reveal about eruption intensity?” Because the origin times of seismic and acoustic transients at Tungurahua appear nearly synchronous (within ~ 1 s), both signals likely result during the onset of explosive degassing. Further degassing, which may reflect continuing foam fragmentation and/or gas bubble rupture, would coincide with the seismic and acoustic codas. From network data, we do not see evidence for synchronous seismo-acoustic sources located external to the conduit system. As a result, we infer that both seismic and acoustic radiation

is primarily produced by acceleration of material within the conduit and vent. Based upon our seismo-acoustic-video observations, we conclude that such accelerations need not be significant to produce a voluminous eruption flux. For example, a simple monopole-type acoustic radiator produces signal proportional to a volumetric acceleration [Lighthill, 1978], which could be negligible for a steady-state flux. A dipole-type acoustic radiator, proposed for gas jetting sources [Woulff and McGetchin, 1975], would also result in diminished acoustic radiation.

[16] In a similar manner, steady laminar flow occurring over a diffuse source region in the conduit might not generate significant changes in traction, which are necessary to generate energetic seismic waves [Aki and Richards, 1980]. It is thus possible to envisage an eruption, which is mostly steady-state and without significant accelerations that is responsible for the low-intensity seismo-acoustic signals recorded in events #3 and 4. Conversely, impulsive eruption onsets at other volcanoes, including Erebus [Rowe et al., 2000] and Stromboli [Ripepe et al., 1996], may exhibit very high-energy seismic-acoustic signatures despite a relative lack of cumulative material emission.

5. Conclusion

[17] Our seismo-acoustic-video study at Tungurahua shows the lack of a clear relation between eruption intensity and elastic energy radiation. Relative timing between the inferred seismo-acoustic source and plume growth provides additional constraints on source mechanisms. We speculate that explosive eruptions can begin impulsively, producing high amplitude seismo-acoustic signals, or may continue in an extended manner as low energy tremor and still result in similarly-sized eruption plumes.

[18] **Acknowledgments.** D. Barba, D. Rivero, and J. Chavez helped in the field. Additional support was provided by H. Yepes, P. Hall, P. Mothes, and many others at the IG-EPN. NSF EAR-0337462, 0440225, 147292, and the Ecuadorian Fulbright Commission supported this work.

References

- Aki, K., and R. Richards (1980), *Quantitative Seismology: Theory and Methods*, 932 pp., W. H. Freeman, New York.
- Chouet, B., N. Hamisevicz, and T. R. McGetchin (1974), Photoballistics of volcanic jet activity at Stromboli, Italy, *J. Geophys. Res.*, **79**, 4961–4976.
- Dibble, R. R., J. Kienle, P. R. Kyle, and K. Shibuya (1984), Geophysical studies of Erebus Volcano, Antarctica, from 1974 December to 1982 January, *N. Z. J. Geol. Geophys.*, **27**(4), 425–455.
- Garces, M. A., M. T. Hagerty, and S. Y. Schwartz (1998), Magma acoustics and time-varying melt properties at Arenal Volcano, Costa Rica, *Geophys. Res. Lett.*, **25**(13), 2293–2296.
- Hagerty, M. T., M. Protti, S. Y. Schwartz, and M. A. Garces (2000), Analysis of seismic and acoustic observations at Arenal Volcano, Costa Rica, 1995–1997, *J. Volcanol. Geotherm. Res.*, **101**(1–2), 27–65.
- Hall, M. L., C. Robin, B. Beate, P. Mothes, and M. Monzier (1999), Tungurahua Volcano, Ecuador: Structure, eruptive history, and hazards, *J. Volcanol. Geotherm. Res.*, **91**(1), 1–21.
- Johnson, J. B. (2000), Interpretation of infrasound generated by erupting volcanoes and seismo-acoustic energy partitioning during Strombolian explosions, Ph.D. thesis, 159 pp., Univ. of Wash., Seattle.
- Johnson, J. B., and R. C. Aster (2005), Relative partitioning of acoustic and seismic energy during Strombolian eruptions, *J. Volcanol. Geotherm. Res.*, in press.
- Johnson, J. B., A. J. L. Harris, S. Sahetapy-Engel, R. E. Wolf, and W. I. Rose (2004), Explosion dynamics of vertically directed pyroclastic eruptions at Santiaguillo Volcano, *Geophys. Res. Lett.*, **31**, L06610, doi:10.1029/2003GL019079.
- Lighthill, M. J. (1978), *Waves in Fluids*, 504 pp., Cambridge Univ. Press, New York.

- McNutt, S. R. (1994), Volcanic tremor amplitude correlated with the Volcanic Explosivity Index and its potential use in determining ash hazards to aviation, *Acta Vulcanol.*, *5*, 193–196.
- Ripepe, M., P. Poggi, T. Braun, and E. I. Gordeev (1996), Infrasonic waves and volcanic tremor at Stromboli, *Geophys. Res. Lett.*, *23*(2), 181–184.
- Ripepe, M., S. Ciliberto, and M. D. Schiava (2001), Time constraints for modeling source dynamics of volcanic explosions at Stromboli, *J. Geophys. Res.*, *106*(B5), 8713–8727.
- Rowe, C. A., R. C. Aster, P. R. Kyle, R. R. Dibble, and J. W. Schlue (2000), Seismic and acoustic observations at Mount Erebus Volcano, Ross Island, Antarctica, *J. Volcanol. Geotherm. Res.*, *101*(1–2), 105–128.
- Ruiz, M., J. M. Lees, and J. B. Johnson (2005), Source constraints of Tungurahua explosion events, *Bull. Volcanol.*, in press.
- Sparks, R. S. J. (1997), *Volcanic Plumes*, 574 pp., John Wiley, Hoboken, N. J.
- Woulff, G., and T. R. McGetchin (1975), Acoustic noise from volcanoes: Theory and experiment, *Geophys. J. R. Astron. Soc.*, *45*, 601–616.
-
- J. B. Johnson, Department of Earth Sciences, University of New Hampshire, Durham, NH 03824, USA. (jeff.johnson@unh.edu)
- J. M. Lees and M. C. Ruiz, Department of Geological Sciences, University of North Carolina, Chapel Hill, NC 27599-3315, USA.
- P. Ramon, Instituto Geofisico, Escuela Politecnica Nacional (IG-EPN), 17-01-2759, Quito, Ecuador.